14th Australasian Fluid Mechanics Conference
Adelaide University, Adelaide, Australia
10-14 December 2001

Characterization of Turbulence Generated by Perforated Plugs of Different Hole Sizes Placed Upstream of a Bunsen Burner

Yung-Cheng Chen and Robert W. Bilger

School of Aerospace, Mechanical and Mechatronic Engineering
University of Sydney, Sydney, New South Wales, 2006 AUSTRALIA

Abstract

The digital particle imaging velocimetry (DPIV) technique is applied to measure simultaneously flow velocity and turbulence integral length scale on a Bunsen burner of 36 mm in diameter. Three perforated plugs of different hole diameters at 2, 4, and 6 mm are used as the turbulence generator placed at 45 mm upstream of the burner exit. The plug opening is controlled to be approximately the same at 55% of the plug surface area. Mean and rms velocities, and the integral length scales are reported at 40 mm downstream of the burner exit

Similar turbulence properties are found for the 4-mm and 6-mm plugs with the decay of centreline rms velocity following the power-law relationship expected for conventional grid-generated turbulence. There is, however, evidence indicating jet coalescence from the holes of the 2-mm plug. The integral length scales do not show clear dependency on the hole diameters of the plugs. This is likely due to low grid Reynolds number as well as intense turbulence, much higher than generated from the plugs, at the shear layer. The current design of turbulence generator requires further improvement for it to be suitable for use in studying low-turbulence premixed flames.

Introduction

Jet flames stabilized on a Bunsen burner are commonly used for laboratory investigations of premixed turbulent combustion. The burner provides good optical access for advanced laser diagnostics probing, and flame stabilization is easily made possible with a small pilot flame around the burner exit. The generation of high turbulence levels is usually achieved by increasing the jet exit velocity to be as high as 65 m/s [2]. This raises the turbulence intensity in the mixing layer, where the mean flame brush may be located. Alternatively, a mesh or perforated plug is inserted at positions upstream of the burner exit [1,6,7]. One advantage of using such grids is that the turbulence level at the burner exit can be adjusted, while the mean flow velocity remains constant. However, performance of these passive devices depends strongly on their design, and detailed characterization is always required for different grids [10]. An attempt is therefore made in this work to study the characteristics of perforated plugs with varied hole diameters.

In previous work [3,4], turbulence intensities and turbulence integral length scales have been measured simultaneously with the DPIV technique. These quantities are important for understanding the different mechanisms of flame-front/flow interactions. It is essential that these turbulence parameters are well controlled and varied in the unburnt mixtures to cover a wide range of experimental conditions. Relatively high turbulence levels have been generated by using perforated plugs at a high blockage ratio [4,5]. The results [5] suggest a new combustion regime of "flame fronts with complex strain" between the turbulent flame-front and laminar flamelet regimes. To investigate turbulent premixed flames in this new regime, low-level turbulence intensity of the same order of the laminar burning velocity or even less is required. It is therefore designed to use perforated plugs with a blockage ratio less than 50%. Turbulence properties using these plugs as turbulence generators are measured with the DPIV technique and reported in this paper.

DPIV System

The current DPIV system consists of a flashlamp pumped, Q-switched, water-cooled Nd:YAG laser (New Wave Research Inc., model Quiklaze), an 8-bit CCD camera (Koda Megaplus, model ES1.0), a PC (Pentium II, 350 MHz), a pulse/delay generator (BNC, model 500B) for timing control, and optical components for laser sheet formation as well as image collection.

The Nd:YAG laser has two laser heads with independent control units so that they can be triggered externally and separately with adjustable time delays. Collimation of the two laser pulses involves only a reflecting mirror and a polarizer. This makes it possible to operate and combine both laser beams at the same second harmonic of 532 nm by using a single frequency-doubling crystal. The energy of each laser pulse is typically 32 mJ and the pulse duration is 6 ns. A beam expander of the reversed Galilean type allows easy adjustment of the laser illumination region depending on the desired imaging area. A cylindrical lens of 200-mm focal length is used to focus the laser beams into thin sheets.

A commercial 55-mm macro lens with a maximum magnification of 1:2 (CCD array to imaging area) is mounted onto the CCD camera to collect particle images. The camera has a CCD array of 1008 X 1018 pixels with each pixel 9 μm square in size. Spatial scaling is determined to be 38.2 pix/mm by imaging a ruler target with the current camera system. The imaging system is also checked in this way to be free from optical distortion. The CCD camera is connected to a frame grabber board installed in a PC and interfaced via the COM port for control commands. External triggering enables synchronization between the laser pulses and the camera operated in the triggered double exposure mode. A minimum of 1 μs is needed between the two exposures to allow the first image to be transferred from the photo diode array to the CCD array. This defines the minimum delay between the two laser pulses. Exposure time of the first image is set to 255 μs; whereas the second image has a fixed exposure period of 9.9 ms. Such long exposure time increases slightly the image background signal (~ 2 to 3 counts) in non-reacting flows, but does not cause any problem in PIV processing.

The software used to control image collection is developed in-house. It waits at background in a loop until the camera receives a trigger signal to activate exposure. After the idle state is again retained, the image buffer on the frame grabber board is automatically transferred into the hard disc. The whole process of image collection is automated, which requires only the initiation of a master trigger by a push-button device or from running in a duty-cycle mode. It takes roughly one hour to complete a data set of 330 image pairs.

Sub-micron "Alu-oxyde" alumina particles are cyclone-seeded in a solenoid-valve controlled air line, which is by-passed from the main air supply. A stable seeding density is optimized by adjusting the by-passed air flow rate. The

solenoid valve and its opening duration are also synchronized with the laser pulse via TTL triggering. The size of most of the particles is less than three pixels on the collected images. Typical signal-to-noise ratio is around 75 to 1.

Particle images are processed with cross-correlation analysis in 64 X 64 pixel interrogation regions of 50% overlap using an optical multichannel analyzer (OMA) code. This software was developed initially by Prof. Long at the Yale University, USA and further enhanced and tested in this laboratory for optimal PIV processing [8]. Instantaneous velocity is determined by dividing the particle displacement by the delay time between two laser pulses, which is 70 μs in this experiment. A 30 X 30 vector field is obtained with each vector representing the average displacement in a 1.67 mm square area. The whole imaging area is approximately 25 mm square. Direct access to the source codes has the additional advantage that specific data reduction procedures can be easily implemented by adding new subroutines, such as for the processing of the two-point correlation functions.

Burner Characteristics

The Bunsen burner used here has an inner diameter of 36 mm. At the burner exit there is a ring of 50 small holes of 1 mm in diameter for the pilot flame. The outer diameter of the burner is 50 mm. The same burner has been used to study flow/flame interactions in this laboratory before [4-7] but with a perforated plug of 78% blockage. In this work, new plugs of a substantially smaller blockage ratio are applied. Adjustment of turbulence characteristics is achieved by moving the perforated plug, which is placed at 45 mm upstream of the burner exit. Detailed dimensions of the plugs are listed in Table 1. The holes are arranged in a hexagonal array with equal spacing between any two adjacent holes. The ratio of hole diameter to hole spacing is kept constant so that the blockage ratio remains approximately the same and less than 50%.

	Plug name		
	Large	Medium	Small
thickness (mm)	10	8	5
hole diameter (mm)	6	4	2
hole spacing (mm)	1.5	1	0.5
blockage ratio	44.6%	45.4%	47.5%

Table 1. Plug characteristics.

The bulk velocity at the burner exit based on the volumetric flow rate, U_o, is chosen to be 5 and 3 m/s. The burner is mounted in a co-flowing air stream at the same velocity of the main jet flow to reduce shear and spreading of the mixing layer. This is intended to generate a turbulent flow field that is still dominated by the burner exit conditions at downstream axial positions.

Flame Heights

The flame heights of lean to stoichiometric CNG/air and LPG/air premixed flames have been determined by visual judgement of the tip of the blue colour. Table 2 shows the measured flame heights. A variation range is given to reflect fluctuations of the flame tip. The flame height depends strongly on the equivalence ratio of unburnt mixtures, ϕ, as well as the mixture exit velocity, U_o. The strong dependency on the equivalence ratio is attributed to the Damköhler number effect: the chemical reaction time increases substantially with a decreasing equivalence ratio. No clear trend can be observed among the three plugs. Therefore, they are not distinguished in Table 2. Also, there appears to be no difference in flame heights for flames using either CNG or LPG as the fuel at the same equivalence ratio, except for the leaner mixtures. The blow-off limit for the exit velocity of U_o = 5 m/s occurs at an equivalence ratio slightly higher than 0.6.

	U_o = 5 m/s	U_o = 3 m/s
CNG/air, ϕ= 1.00	8 - 15 cm	5 - 10 cm
CNG/air, ϕ = 0.85	12 - 18 cm	8 - 12 cm
CNG/air, ϕ = 0.70	21 - 34 cm	13 - 24 cm
CNG/air, ϕ = 0.60	blow-off	25 - 43 cm
LPG/air, ϕ = 1.00	9 - 15 cm	6 - 10 cm
LPG/air, ϕ = 0.85	12 - 19 cm	9 - 13 cm
LPG/air, ϕ = 0.70	22 - 34 cm	18 - 28 cm
LPG/air, ϕ = 0.60	blow-off	29 - 46 cm

Table 2. Measured flame heights.

Based on the above flame height data, PIV measurements are conducted from x = 40 mm to 65 mm, and r = -5 mm to 20 mm in non-reacting flows. This imaging position is chosen for ease of comparison with future conditional velocity measurements in the flames using the joint PIV/OH-LIF technique. In the following, mean and turbulence quantities for U_o = 5 m/s are presented at an axial position of x = 40 mm.

Mean and RMS Velocity

The radial profiles of the axial and radial mean velocities are shown in Figure 1 at x = 40 mm downstream of the burner exit. Velocities are normalized by the bulk velocity at the burner exit of 5 m/s. The radius is normalized by the burner diameter of D = 36 mm. A close-to flat-top profile of the axial mean velocity is found at r/D < 0.2 for the large and medium plugs. This feature suggests that the flow field near jet centerline is still subject to the turbulence generators. On the other hand, the small plug shows a marked dent in the axial mean velocity profile at the jet centreline. Also, the radial mean velocity in this region is almost zero. This anomalous behaviour is likely to be due to jet coalescence in the small plug having holes too close to each other.

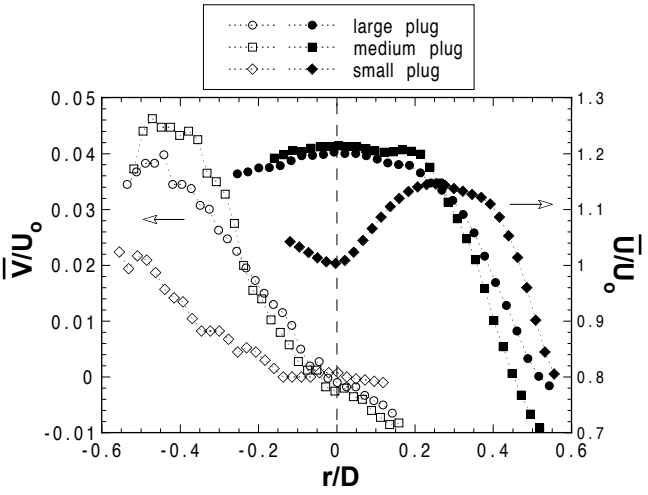

Figure 1. Axial and radial mean velocities at x = 40 mm.

The radial profiles of the axial and radial root mean square (rms) velocities are shown in Figure 2 at x = 40 mm downstream of the burner exit. Turbulence intensity decreases when the diameter of holes in the plug decreases from 6, 4 to 2 mm. Turbulence intensity normalized by the mean velcoity, $u'/\overline{U}$, also decreases from 6.0%, 5.5%, to 5.0% at the jet centreline. For reference, the relative turbulence intensity measured without any plug is approximately 7.5% for the current Bunsen burner. Thus, the turbulence declines when inserting the perforated plugs. And the reduction of turbulence

levels scales inversely with the hole diameter in the plug. As expected, these turbulence levels are comparatively lower than those from previous measurements [4] using plugs of a much larger blockage ratio of more than 75%. A gently undulating distribution of the turbulence intensity is found near the jet centreline for the small plug, and is possibly associated with the coalescing of the jets from individual holes of this plug.

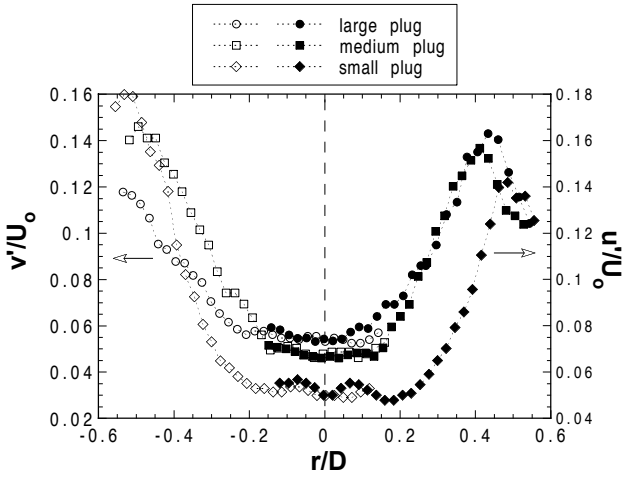

Figure 2. Axial and radial rms velocities at x = 40 mm.

A substantial increase of the rms velocity is, however, observed from r/D = 0.2 to 0.55 in Figure 2, suggesting intense shear layer turbulence at the measuring station. For the flames listed in Table 2, the mean flame brush position is most likely to be located near the shear layer. The local flame structure therefore may depend strongly on the shear layer turbulence, which is not fully controlled by the perforated plugs.

PIV Measurements have been further conducted at conditions where the medium plug is placed at several different upstream locations. Figure 3 shows the variation of the centreline turbulence intensities. The PIV data agree reasonably well with separate LDV measurements. X_p is the distance from the plug location to the measuring station, which is fixed at 40 mm above the burner exit. Both u' and v' decrease quickly when the plug is moved upstream. The decay rates of both u'/U_o and v'/U_o versus X_p can be curve-fitted with a power-law relationship for X_p < 130 mm. The derived exponent is 0.63 and is almost the same for u' and v' rms velocity. This number is very close to 0.65, reported elsewhere for grid-generated turbulence [9]. After the plug is moved to be more than 90 mm from the burner exit (X_p > 130 mm), turbulence intensities become almost independent of the plug position.

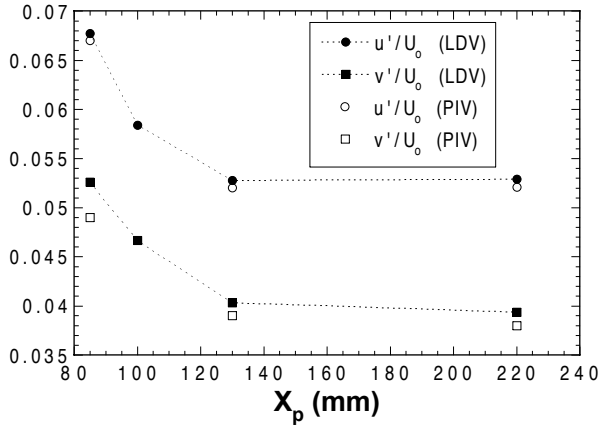

Figure 3. Variation of centreline rms velocities using the medium plug.

Integral Length Scales

Previous studies conducted in this laboratory [3,4] have demonstrated that in additional to turbulence intensities, satisfactory measurements of the turbulence integral length scale can also be obtained from the PIV data. The two-point longitudinal correlation functions, $f(\Delta x;r_o)$, of the axial velocity component at point (x_o,r_o) are derived using Equation (1) from 330 processed instantaneous PIV velocity fields.

$$f(\Delta x;r_o)=\frac{\overline{u(x_o,r_o)\,u(x_o+\Delta x,r_o)}}{u'(x_o,r_o)\,u'(x_o+\Delta x,r_o)} \qquad (1)$$

Δx is the increasing axial distance between two velocity vectors at the radial position of $r = r_o$. Figure 4 shows the correlation functions (in symbols) measured at two radial positions using the small plug. The solid lines are obtained from curve-fitting of data points with the following formula

$$f(\Delta x;r_o)=a\left(1-\frac{b\Delta x}{2}\right)e^{-b\Delta x}+c\left(1-\frac{d\Delta x}{2}\right)e^{-d\Delta x} \qquad (2)$$

At r = 10 mm, $f(\Delta x;r_o)$ decreases quickly to be almost zero and increases again with increasing Δx. At this radial position, the low-turbulence potential core starts to interact with intense shear-layer turbulence. The unusually high correlation in Figure 4(b) at large Δx seems to indicate generation of organized vortex structures along the interaction boundary. Curve-fit using Equation (2), however, takes only those data points that are decreasing monotonically, *i.e.*, Δx < 12 mm. It is also noted that Equation (2) does not guarantee a total correlation when Δx = 0. However, the deviation of $f(\Delta x;r_o)$ at Δx = 0 is always within 5% throughout the present measurements.

The integral length scale can then be obtained using either integrating directly the area underneath the measured two-point correlation functions shown in Figure 4 or using the curve-fit formula, equation (2), such that

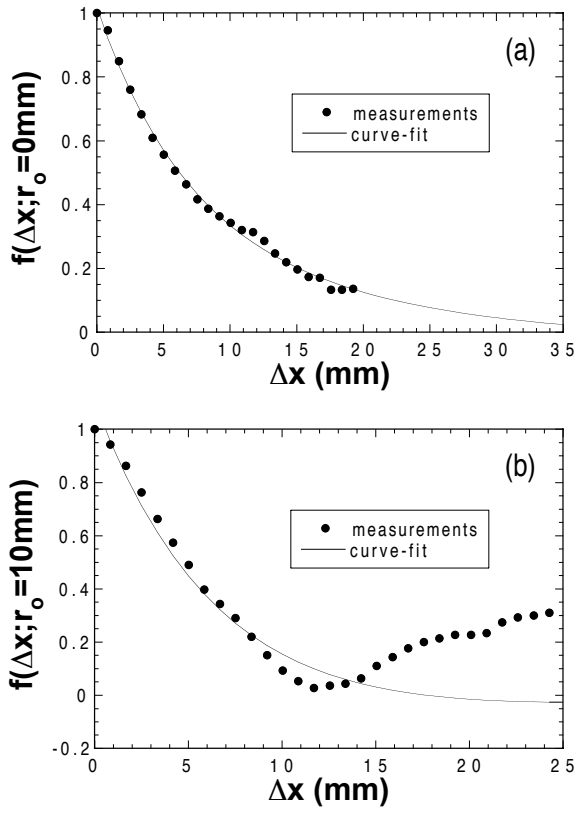

Figure 4. Two-point longitudinal correlation functions at (a) x_o = 40 mm, r_o = 0 mm; and (b) x_o = 40 mm, r_o = 10 mm.

$$\ell_f = \frac{a}{2b} + \frac{c}{2d} \quad (3)$$

The longitudinal integral length scales, ℓ_f, obtained with Equation (3) are shown in Figure 5 for the three plugs. The radial profiles of ℓ_f for the medium and large plugs are almost the same in Figure 5, so are the turbulence intensities in Figure 2. This seems to suggest that the turbulent properties generated from these two plugs are developing quickly into similar distributions, except for the v' component of the rms velocity. A slightly different behaviour of the longitudinal integral length scale is found for the small plug, which shows a maximum at the jet centreline, and relatively smaller values at larger radius.

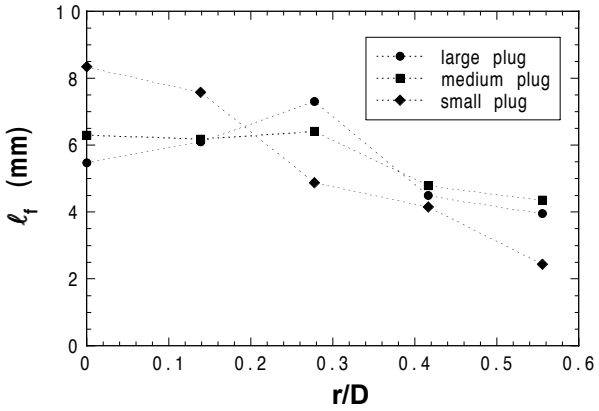

Figure 5. Radial profiles of the longitudinal integral length scale measured at x = 40 mm.

Measurements are further made closer to the burner exit to reveal the axial evolution of the integral length scales for the large plug. Figure 6 shows that ℓ_f is almost a constant of 4 mm at x = 5 mm. Above this height, ℓ_f decreases at the jet centreline as well as near the mixing layer and increases for r between 5 and 10 mm. A similar radial distribution of ℓ_f is maintained from this height above up to x = 40 mm, whereas the absolute values increase further by approximately 25%. This indeed implies a fairly quick development of the integral length scales above the burner exit.

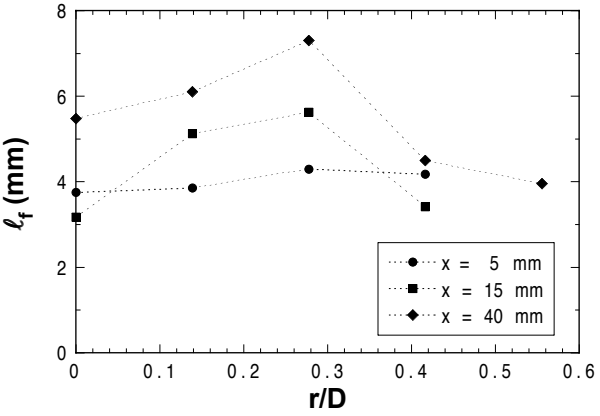

Figure 6. Radial profiles of measured longitudinal integral length scales at several axial locations for the large plug placed at 45 mm upstream.

No clear dependency can be inferred of the measured integral length scale on the hole diameter of the plugs in Figure 5. It is likely that the grid Reynolds numbers are too low in this experiment, with values less than 2500 based on the mesh size (hole diameter + spacing). Anomalous behaviours with shear layer instability and remnant upstream background turbulence have been reported [11] with perforated plates of the same order of grid Reynolds numbers. Also, much higher turbulence generated along the shear layer may reduce substantially the length of the potential core and contribute to the quick increase of the integral length scale above the burner exit as suggested in Figure 6.

Conclusions

Turbulence properties have been measured with the PIV technique at 40 mm downstream of a Bunsen burner inserted with plugs having different hole diameters. Turbulence intensities near the jet centreline are found to be close to grid-generated turbulence for the large and medium plugs. However, no clear dependency is observed of the longitudinal integral length scale on the hole diameter. This is likely due to low grid Reynolds numbers as well as intense shear-layer turbulence, such that the integral length scale increases rapidly at positions above the burner exit.

Flame heights of lean to stoichiometric CNG/air and LPG/air premixed flames stabilized on this burner have also been determined. They vary considerably with the equivalence ratio, or the associated chemical time scale. No clear dependency on the plugs is observed, consistent with the moderate range of turbulence intensity that is measured. Despite the low turbulence intensities obtained, the current design of turbulence generator with perforated plugs needs improvement to achieve design goals.

Acknowledgments

This work is supported by the Australian Research Council.

References

[1] Buschmann, A., Dinkelacker, F., Schäfer, M., & Wolfrum, J., Measurement of the Instantaneous Detailed Flame Structure in Turbulent Premixed Combustion, *Proc. Combust. Inst.*, **26**, 1996, 437-445.

[2] Chen, Y.-C., Peters, N., Schneemann, G.A., wruck, N., Renz, U., & mansour, M.S., The Detailed Flame Structure of Highly Stretched Turbulent Premixed Methane-Air Flames, *Combust. Flame*, **107**, 1996, 223-244.

[3] Chen, Y.-C., Kalt, P.A.M., Masri, A.R. & Bilger, R.W., Feasibility Study of Integral Length Scale Measurements in Turbulent Jet Flows Using DPIV, in *Proceedings of The 2nd Australian Conference on Laser Diagnostics in Fluid Mechanics and Combustion*, editors J. Soria and D. Honnery, Monash University Printing Services, 1999, 57-61.

[4] Chen, Y.-C. & Bilger, R.W., Simultaneous 2-D Imaging Measurements of Reaction Progress Variable and OH Radical Concentration in Turbulent Premixed Flames: Experimental Methods and Flame Brush Structure, *Combust. Sci. & Technol.*, 2001 (to appear).

[5] Chen, Y.-C. & Bilger, R.W., Simultaneous 2-D Imaging Measurements of Reaction Progress Variable and OH Radical Concentration in Turbulent Premixed Flames: Instantaneous Flame Structure, *Combust. Sci. & Technol.*, 2001 (to appear).

[6] Frank, J.H., Kalt, P.A.M., and Bilger, R.W., Measurements of Conditional Velocities in Turbulent Premixed Flames by Simultaneous OH PLIF and PIV, *Combust. Flame*, **116**, 1999, 220-232.

[7] Kalt, P.A.M., Frank, J.H., and Bilger, R.W., Laser Imaging of Conditional Velocities in Premixed Propane-Air Flames by Simultaneous OH PLIF and PIV, *Proc. Combust. Inst.*, **27**, 1998, 751-758.

[8] Kalt, P.A.M., & Masri, A.R., Development of a Low-Cost and Modular Digital Cross-Correlation PIV System, in *Proceedings of The 2nd Australian Conference on Laser Diagnostics in Fluid Mechanics and Combustion*, editors J. Soria and D. Honnery, Monash University Printing Services, 1999, 44-49.

[9] Mohamed, M.S. & LaRue, J.C., The decay power law in grid-generated turbulence, *J. Fluid Mech.*, **219**, 1990, 195-214.

[10] Roach, P.E., The generation of nearly isotropic turbulence by means of grids, *Int. J. Heat and Fluid Flow*, 8, 1986, 82-92.

[11] Tan-atichat, J., Nagib, H.M., & Loehrke, R.I., Interaction of Free-Stream and Grids: a Balance Between Turbulence Scales, *J. Fluid Mech.*, **114**, 1982, 501-528.